IET Microwaves, Antennas & Propagation

Research Article

IET Journals
The Institution of Engineering and Technology

Compact tunable bandpass filter with wide tuning range of centre frequency and bandwidth using coupled lines and short-ended stubs

ISSN 1751-8725
Received on 27th October 2015
Revised on 29th January 2016
Accepted on 28th February 2016
doi: 10.1049/iet-map.2015.0693
www.ietdl.org

He Zhu ✉, *Amin Abbosh*

School of ITEE, The University of Queensland, St Lucia, Brisbane, Queensland 4072, Australia
✉ *E-mail: h.zhu5@uq.edu.au*

Abstract: A tunable bandpass filter with wide tuning range of both its centre frequency and bandwidth is presented. This type of filter is a key element in modern wideband and multiband systems. The proposed filter is based on short sections of two pairs of shunt connected parallel-coupled lines and short-ended stub resonators, which are tuned using varactor diodes. The structure has two resonant modes as well as one-side edge transmission zero that can be relocated and controlled for any desired position. A thorough theoretical analysis is utilised to find the initial values of the filter's design parameters and estimate its performance. To validate the proposed design and its theoretical analysis, two prototype filters are fabricated and tested. The measured results indicate wide tuning range ratios for the centre frequency and bandwidth of up to 2.85 (0.52 to 1.48 GHz) and up to 5.2 (55 to 285 MHz), respectively. The fabricated filters are compact with an overall size (in guided wavelengths at the centre frequency) of less than 0.06×0.16.

1 Introduction

Tunable bandpass filters (BPFs) are key elements in modern generations of multiband and wideband systems due to their reconfigurable performance, reduced complexity, compact size, and low cost. Such kinds of components are greatly demanded in many RF front-ends, such as wireless communication, near-body medical imaging systems, and cognitive radios [1–5].

Usually tunable BPFs can be classified based on their reconfigurability into three main types: tunable bandwidth with fixed centre frequency [6, 7]; tunable centre frequency with constant bandwidth [8–14]; and tunable bandwidth as well as centre frequency [15–22]. Among all these three types, the third one is the most needed and used due to the flexibility that it can offer when used in wideband or multiband systems especially if the utilised filters have wide tuning range for both the centre frequency and bandwidth. To realise that target, different kinds of resonators were investigated and adopted. Notable examples of the used resonators include cascaded structures [15], comb-lines [16–18], patch [19], loop-shaped [20], multi-mode resonator [21], square-loop slot [22], open-stub loaded half-wavelength resonators [23], and ring resonator [24]. When designing tunable BPFs, creating controllable and adjustable transmission zeros for better selectivity is another important issue of the design. Examples of the structures that tackled that issue include using varactors loaded dual-mode microstrip open-loop resonator [25], stub-loaded resonators [26] and T-shaped dual-mode resonator [27]. Moreover, a new class of reconfigurable filters [28, 29] which is capable of realising arbitrary number of passbands with tune-all capability has been recently introduced; however, it could be difficult to apply these designs in practice due to the large number of required capacitances.

In reviewing the aforementioned designs, it is clear that a research challenge still remains on whether one simple structure with a significantly small size can be used to realise a wide tuning range for both of the bandwidth and centre frequency with reconfigurable transmission zeros. To that end, this paper aims at building a simple and compact tunable BPF that has a wide tuning range of both the bandwidth and centre frequency with sharp selectivity using a compact structure of single-layer microstrip technique. To realise that target, an innovative design approach, which utilises a compact two-pole short-ended stub-loaded resonator, is proposed. The utilised design aims at realising a full control of the location of transmission poles and zeros, and coupling of the passband. Thus, the design can achieve a full bandwidth and centre frequency tunability. Once the circuit parameters and design targets (such as location of transmission zeros, in-band attenuation level, bandwidth etc.) are determined, the required values of all the tuning elements can be obtained. A thorough analysis of the circuit and its design procedure are given. To verify the proposed design, two structures with different locations of transmission zeros, are designed and tested. Compared with the reported works, the proposed design achieves an extremely wide tuning range for both of centre frequency (from 0.52 to 1.48 GHz) and bandwidth (from 55 up to 285 MHz) as well as an adjustable one-edge transmission zero using the mots compact single-layer structure.

2 Proposed tunable BPF

2.1 Analysis

Fig. 1*a* shows a schematic diagram of the proposed tunable BPF. It is composed of a short-ended coupled-line section, which has even- and odd-mode admittances of Y_{oe}, Y_{oo} and electrical length of θ_o, calculated at the centre frequency f_c, connected in parallel with a pair of short-ended stubs, which have an admittance of Y_1 and electrical length of θ_1, calculated at f_c. Several varactors that have the following capacitances are added to the structure at different locations to control the filtering performance: two pairs of varactors with capacitances C_1 and C_2 forming two inverted L-sections that connect the input and output ports to the resonator; and a varactor with a capacitance C_3 connected between the coupled-line section and stubs.

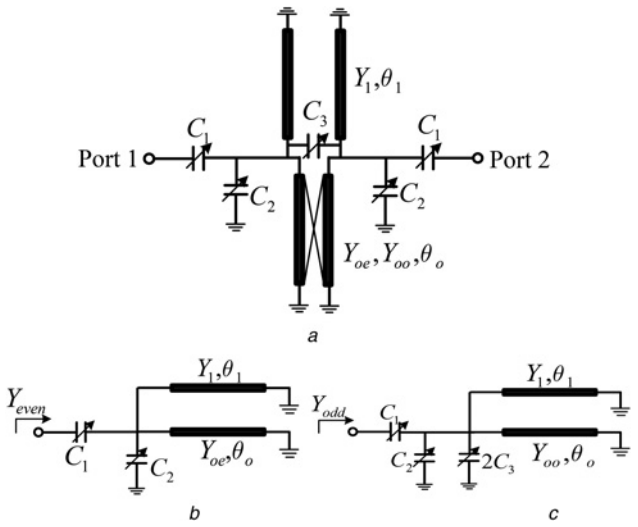

Fig. 1 *Schematic diagram of the proposed tunable BPF*

a Transmission line schematic of the proposed filter
b Even-mode equivalent circuit
c Odd-mode equivalent circuit

Since the proposed structure in Fig. 1*a* is symmetric, the even-/odd-mode analysis method can be adopted. To that end, the even- and odd-mode equivalent circuits of the proposed filter are given in Figs. 1*b* and *c*. For the even-mode case, the input admittance is

$$Y_{\text{even}} = \frac{j\omega C_1 \cdot (j\omega C_2 - jY_1 \cot\theta_1 - jY_{\text{oe}} \cot\theta_0)}{j\omega C_1 + j\omega C_2 - jY_1 \cot\theta_1 - jY_{\text{oe}} \cot\theta_0} \tag{1}$$

The odd-mode input admittance is

$$Y_{\text{odd}} = \frac{j\omega C_1 \cdot (j\omega C_2 + j2\omega C_3 - jY_1 \cot\theta_1 - jY_{\text{oo}} \cot\theta_0)}{j\omega C_1 + j\omega C_2 + j2\omega C_3 - jY_1 \cot\theta_1 - jY_{\text{oo}} \cot\theta_0} \tag{2}$$

Assuming that the device is connected to ports that have a characteristic admittance (Y_o), the scattering parameters of the structure in Fig. 1 can be calculated from the admittance parameters.

$$S_{11} = \frac{Y_o^2 - Y_{\text{odd}}Y_{\text{even}}}{(Y_o + Y_{\text{odd}})(Y_o + Y_{\text{even}})} \tag{3}$$

$$S_{21} = \frac{Y_o(Y_{\text{odd}} - Y_{\text{even}})}{(Y_o + Y_{\text{odd}})(Y_o + Y_{\text{even}})} \tag{4}$$

The overall performance of the BPF can thus be calculated using (3) and (4). Based on the targeted fractional bandwidth (FBW) and centre frequency f_c, a tunable BPF can be constructed when the resonant frequencies f_{even} and f_{odd} are known. It is known that the even- and odd-mode resonant frequencies of the structure can be found from the following conditions

$$\text{Im}[Y_{\text{even}}] = 0 \tag{5}$$

$$\text{Im}[Y_{\text{odd}}] = 0 \tag{6}$$

Solving (5) and (6) and using (1) and (2), the relation between the resonant frequencies (f_{even} and f_{odd}) and the design parameters of the filter can be expressed as

$$f_{\text{even}} = \frac{Y_1 \cot\theta_1 + Y_{0\text{e}} \cot\theta_0}{2\pi \cdot \left(C_2 + \left(C_1/1 + (\omega C_1/Y_0)^2\right)\right)} \tag{7}$$

$$f_{\text{odd}} = \frac{Y_1 \cot\theta_1 + Y_{0\text{o}} \cot\theta_0}{2\pi \cdot \left(C_2 + 2C_3 + \left(C_1/1 + (\omega C_1/Y_0)^2\right)\right)} \tag{8}$$

From (7) and (8), it is observed that f_{even} depends on C_1, C_2, and has nothing to do with C_3, while f_{odd} is related to C_1, C_2 and C_3 at the same time. Since f_{even} and f_{odd} defines the tuning range for both of the band and centre frequency, it is possible to conclude from (7) and (8) that the varactor capacitances C_1–C_3 can be used to tune the centre frequency and band of the filter. The criteria of selecting these capacitances are given in the following sections.

2.2 Transmission zeros

To achieve sharp selectivity of the passband, the transmission zeros of the filter are to be properly located. To find the location of those transmission zeros, the condition $|S_{21}| = 0$ is to be solved. From (6), it is possible to conclude that the aforementioned condition can be met with the following cases.

$$Y_{\text{odd}} - Y_{\text{even}} = 0 \tag{9}$$

$$\begin{cases} |Y_{\text{even}}| = \infty \\ |Y_{\text{odd}}| = \infty \end{cases} \tag{10}$$

The solution of (9) gives the location of the transmission zero f_{tz1}, which can be made very close to the passband for better selectivity.

$$f_{\text{tz1}} \cdot \tan\left(\theta_0 \frac{f_{\text{tz1}}}{f_0}\right) = \frac{(Y_{\text{oo}} - Y_{\text{oe}})}{4\pi C_3} \tag{11}$$

From (11) one can find that the position of f_{tz1} is determined by the properties of the coupled-line section (Y_{oe}, Y_{oo}, and θ_0) and the capacitance C_3. It is observed that when $f_{\text{even}} > f_{\text{odd}}$, f_{tz1} appears at the upper side of the passband, but when $f_{\text{even}} < f_{\text{odd}}$, f_{tz1} appears at the lower side of the passband. Those two cases are fully controlled using C_3, as proven in (11), enabling the reconfigurability of this effective transmission zero in line with the centre and band tunability as required by the design. The other transmission zeros, which can be found by solving (10), are expressed as

$$f_{\text{tz2}} = \frac{n\pi f_c}{\theta_0}, \quad n = 0, 1, 2\ldots \tag{12}$$

$$f_{\text{tz3}} = \frac{n\pi f_c}{\theta_1}, \quad n = 0, 1, 2\ldots \tag{13}$$

Obviously, a transmission zero appears at DC when n equals to zero. The first two non-zero TZs occur when n equals 1. As observed from (12) and (13), the smaller θ_0 and θ_1 are, the larger f_{tz2} and f_{tz3} will be. Therefore, with the aim of achieving a compact structure and thus using small values for θ_0 and θ_1, these two transmission zeros will be located at higher frequencies, resulting in good suppression of harmonics in the upper-stopband at selected locations as per (12) and (13). Besides, these two transmission zeros are not affected by the varactor capacitances, indicating the possibility for the designer to locate them appropriately to suppress any harmonics irrespective of the tuning requirement.

2.3 Filter tunability

To judge the required values of the design parameters needed for a certain tunability range of the filter concerning its centre frequency and bandwidth, let us assume that a filter with the following requirements are needed. Centre frequency tuning range is from 0.5 to 1.5 GHz, and bandwidth range is from 50 to 250 MHz. Using the iterative solution of the previous theory, it is possible to find that the following values of the design parameters are needed: $\theta_0 = \theta_1 = 30°$, $Z_{\text{oe}} = 1/Y_{\text{oe}} = 160\ \Omega$, $Z_{\text{oo}} = 1/Y_{\text{oo}} = 65\ \Omega$, and $Z_1 = 1/Y_1 = 100\ \Omega$. Using parametric analysis for other design requirements, it was found that the values of Z_{oe}, Z_{oo} and Z_1

IET Microw. Antennas Propag., 2016, Vol. 10, Iss. 8, pp. 863–870

should meet the following conditions.

$$\sqrt{Z_{oe}Z_{oo}} = 2Z_o = 100\,\Omega \tag{14}$$

$$Z_1 = 2Z_o = 100\,\Omega \tag{15}$$

Using those calculated values in (7), (8) and (11), variation of the resonant frequencies (f_{even} and f_{odd}) and transmission zero f_{tz1} for different values of the varactor capacitances are calculated and shown in Fig. 2. It can be easily concluded from the results that two resonant modes are utilised in the filter design. From Fig. 2*a*, one can find that C_1 has no effect on f_{tz1}, as previously expected, and has a slight effect on f_{odd} and f_{even}. From Fig. 2*b*, it is also possible to conclude that when C_2 is increased, both of f_{odd} and f_{even} decrease, while the transmission zero f_{tz1} remains constant. When C_3 is changed, f_{odd} remains constant, while f_{even} and f_{tz1} vary significantly, as observed in Fig. 2*c*. It is noted that the intersection points, such as the points P and Q in Figs. 2*b* and *c*, indicate the case when the three frequencies (f_{even}, f_{odd}, f_{tz1}) have the same value. It is well known that the even- and odd-mode resonant frequencies have the following relation with the filter's centre frequency

$$f_c = \frac{f_{even} + f_{odd}}{2} \tag{16}$$

Thus, it is possible to conclude that the intersection points P and Q in Fig. 2 actually indicate the case of locating the TZ at the position of the centre frequency. Thus, this case represents an all-reject filter and it is a transitional case that marks the values of the varactor capacitance that cause a shift in the position of f_{tz1} from the upper to the lower side of the passband. This case is important in the design in the sense that it represents the possibility of the transmission zero relocation.

Using the selected circuit parameters in (7) and (8) with varactor capacitance that changes within the reasonable range (e.g. 0.3–15 pF), the scattering parameters of the filter can be calculated as depicted in Fig. 3*a*–*c*. In Fig. 3*a*, the centre frequency of the operating band can be shifted from 0.5 to 1.5 GHz, with fixed bandwidth and f_{tz1} located at the upper side of the passband; while from Fig. 3*b*, same performance is achieved except the transmission zero is located at the lower side of the passband. Bandwidth tunability is shown in Fig. 3*c* demonstrating a tunable 3-dB bandwidth from 50 to 300 MHz at certain frequency. The value range of capacitance used in all cases is from 0.3 to 15 pF, which can be realised by RF varactors. These results reveal the potential of the proposed structure to realise a wide range of tunability for the centre frequency and bandwidth as well as a relocatable transmission zero. It is also noted that by appropriately selecting the values of C_1, C_2 and C_3 to meet the aforementioned situation $f_{even} = f_{odd} = f_{tz1}$, the passband is suppressed by the transmission zero, resulting in zero bandwidth of the passband as shown in Fig. 3*d*.

To further improve the selectivity of passband, the proposed structure can be extrapolated to higher order. For an n-order filter, there are n-1 transmission zeros appearing at the edges and n transmission poles within the passband. To increase the order of the presented basic structure, additional short-ended stubs with equal length can be added to the coupled-line section. Moreover, an additional varactor is connected between any two adjacent stubs, such as C_3 in Fig. 1, while C_1 and C_2 remain the same for the two-order filter. Meanwhile, an additional varactor is needed at the end of the stubs which are not the first or the last one. This is because more controllability of the resonant mode is required when tuning the position of passband. In this way, the external quality factor and coupling coefficients can be easily controlled. By upgrading the proposed structure to higher order ($n \geq 3$), more transmission zeros and poles can be achieved, which is favourable for sharper passband selectivity and better stopband rejection. Here, a three-pole structure, which has full tunability of bandwidth and operating frequency, is included as an example, as shown in Fig. 4*a*.

It is observed from Fig. 4*a* that three-pole structure is composed of a three-line coupled-line section, two short-ended stubs and an open-ended stub in the middle. All the stubs have the same length of θ_s, while the coupled-line section's length is θ_0. To control the filtering performance, two pairs of varactors with capacitances C_1 and C_2 forming two inverted L-sections that connect the input and output ports to the resonator, and a varactor with a capacitance C_3 connected between the coupled-line section and stubs are used. An additional varactor C_4 is added at the end of the middle-line. Figs. 4*b* and *c* show the tunability of the three-pole BPF. By increasing the capacitance of C_1, C_2, C_3, and C_4, the operating frequency moves to higher frequencies. Two transmission zeros are created at one side of the passband, and can be shifted to the other side of the passband. Due to the existence of C_2, C_3, and C_4, all the three resonant modes can be fully controlled. Meanwhile, the external quality factor is controlled by C_1, and thus the operating bandwidth can be increased or reduced as needed. Compared with the performance of the two-pole structure (Fig. 3), the three-pole design has sharper cut-off and thus better selectivity

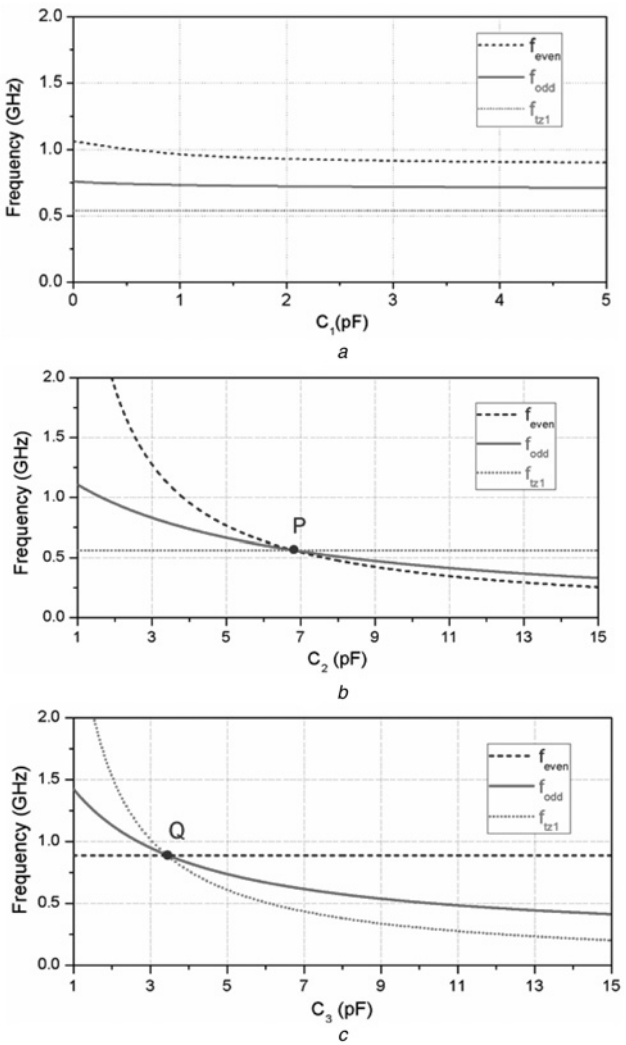

Fig. 2 *Relation between resonant frequencies (f_{even}, f_{odd}), transmission zero (f_{tz1}) and the capacitances*

a C_1
b C_2
c C_3

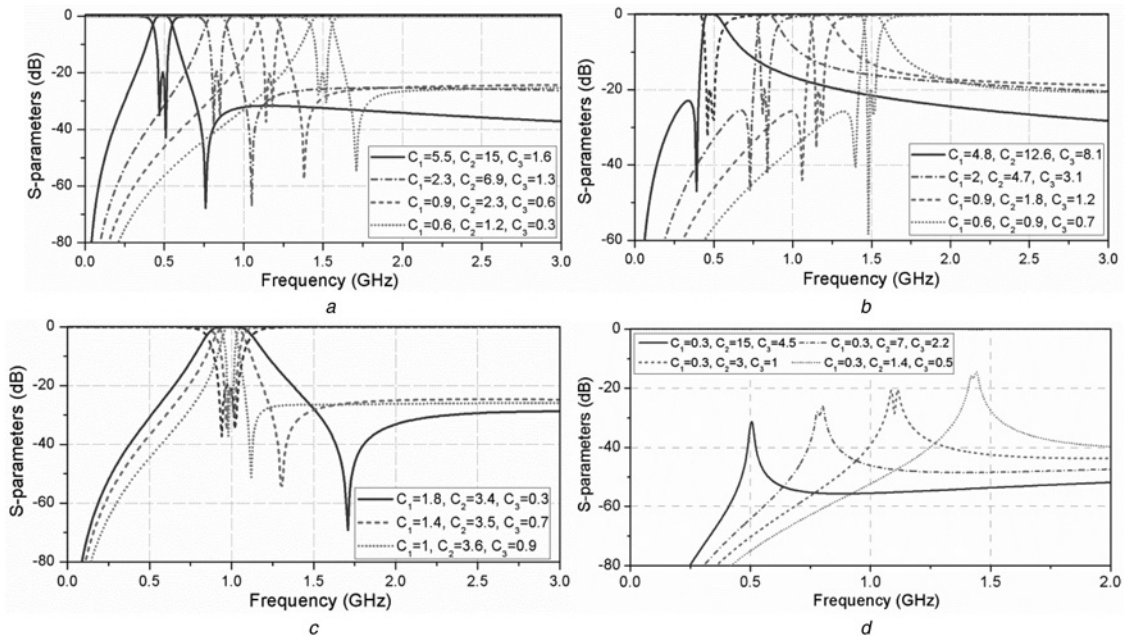

Fig. 3 *Calculated performance for*

a Tunable centre frequency with upper side transmission zero
b Tunable centre frequency with lower side transmission zero
c Tunable bandwidth
d Zero-bandwidth situation (unit: pF)

as depicted in Figs. 4*b* and *c*. Since this paper is focused on second-order filter design, a detailed design procedure is listed in the next section, followed by experimental verification of two design examples.

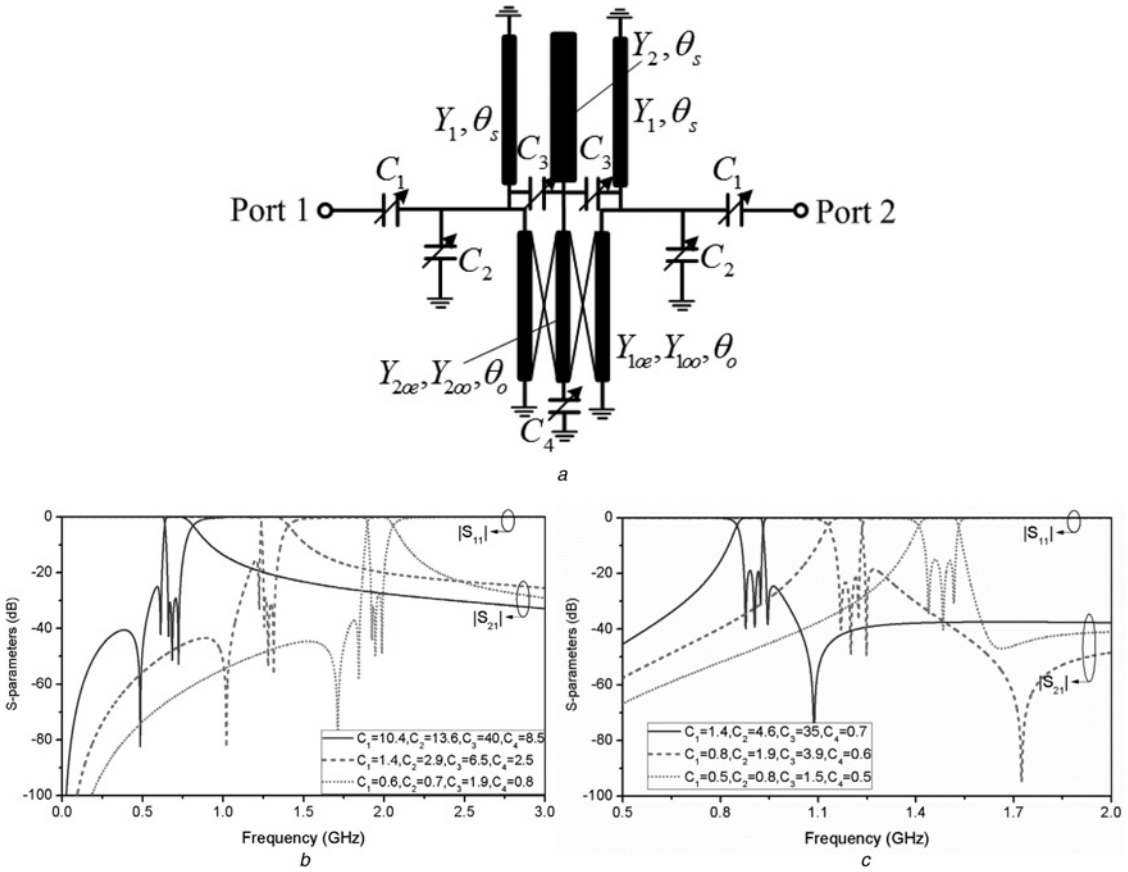

Fig. 4 *Third-order tunable bandpass filter*

a Transmission-line schematic of the third-order tunable BPF
b Tunable filtering response of the third-order BPF with transmission zeros at left side
c Tunable filtering response of the third-order BPF with transmission zeros at right side

IET Microw. Antennas Propag., 2016, Vol. 10, Iss. 8, pp. 863–870

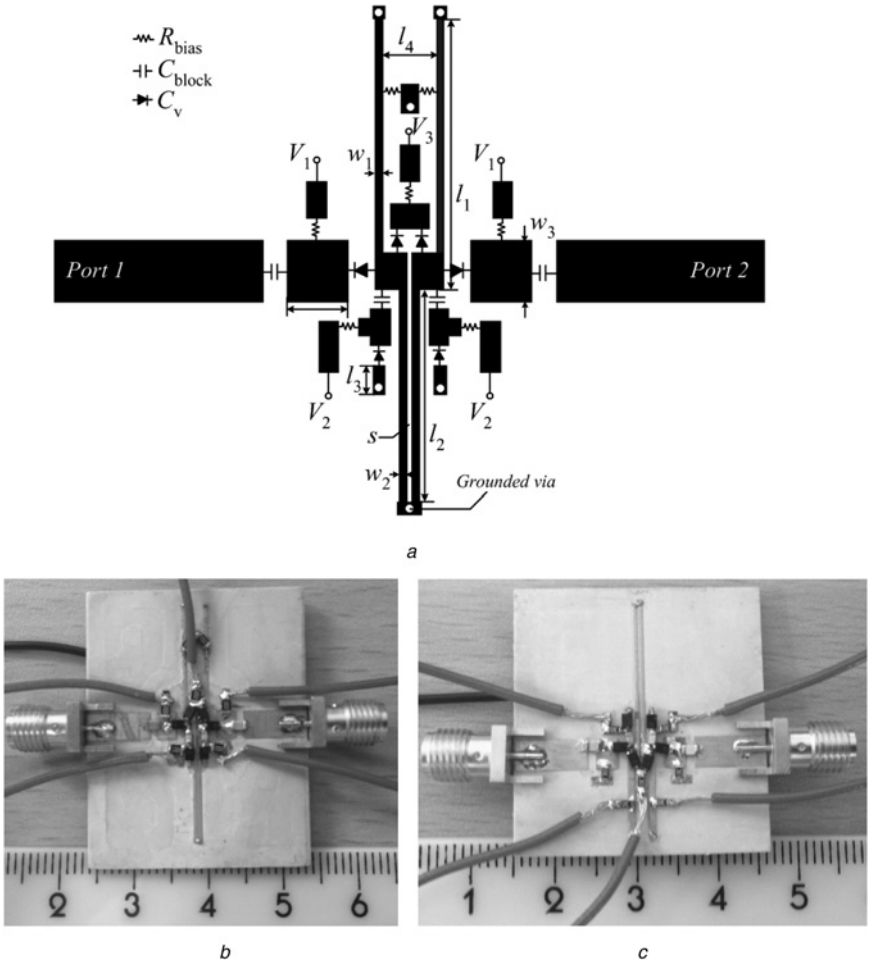

Fig. 5 *Configuration of the proposed tunable BPF*

a Layout of the proposed tunable BPF
b Photos of the fabricated prototype filter Design #1
c Photos of the fabricated prototype filter Design #2

3 Design procedure

Assume it is required to design a BPF filter with certain average objectives for the centre frequency f_c and FBW. The design then proceeds with following steps using the proposed structure:

(i) Select a target tuning range of centre frequency f_c and FBW. As an example in this design, the target is set as centre frequency tunability from 0.5 to 1.5 GHz ($f_c = 1$ GHz), and bandwidth from 50 to 150 MHz.

(ii) Choose appropriate lowpass filter prototype with the desired in-band attenuation level and bandwidth, find its basic element values (g_x) and then obtain the values of the coupling coefficient k and external quality factors Q_{ex} using the following equations [30]

$$k_{12} = \frac{\text{FBW}}{\sqrt{g_1 g_2}} \tag{17}$$

$$Q_{ex} = \frac{g_0 g_1}{\text{FBW}} \tag{18}$$

(iii) On the basis of the average design objectives (centre frequency and average bandwidth), select the locations of the transmission zeros f_{tz2} and f_{tz3}, and then calculate the required values for θ_0, and θ_1 using (12) and (13). Usually, the lengths of the short-ended stubs and coupled-lines are selected as around on-fifth to one-third of quarter-wavelength at f_c. Based on our parametric investigation, Z_1 is fixed at 100 Ω, Z_{oo} is selected between 60 and 80 Ω, and $Z_{oe} = 4Z_0/Z_{oo}$.

(iv) The initial values for C_1, C_2, and C_3 are selected, usually between 0.5 and 15 pF, using an iterative solution to meet (i) the desired position of the transmission zero from (11), (ii) the (7) and (8) so that $f_{even} > f_c > f_{odd}$, if f_{tz1} appears at the upper side of the passband; $f_{odd} > f_c > f_{even}$, if f_{tz1} appears at the lower side of the passband, and (iii) the calculated coupling coefficient k and external quality factors Q_{ex} from step (ii) as per the following equations [11]

$$k_{12} = \frac{\text{Im}\left[Y_{\text{even}}(\omega_0) - Y_{\text{odd}}(\omega_0)\right]}{2b} \tag{19}$$

$$Q_{ex} = \frac{(\omega_0/2) \cdot \left(\partial \text{Im}\left[Y_{\text{in}}(\omega_0)\right]/\partial\omega\right)}{Y_0} \tag{20}$$

where

$$b = \frac{\omega_0}{4} \cdot \frac{\partial \text{Im}\left[Y_{\text{even}}(\omega_0) + Y_{\text{odd}}(\omega_0)\right]}{\partial\omega} \tag{21}$$

(v) Use (1)–(4) to calculate the S-parameters of the filter. In this case, the performance may not perfectly match the required design requirements due to the non-linear nature of the design equations. If that is the case, the iterative solution of step (iv) is repeated to

Table 1 Values of design parameters (dimensions in mm)

Design #1				Design #2			
Name	Value	Name	Value	Name	Value	Name	Value
l_1	17.2	w_1	0.3	l_1	10.6	w_1	0.8
l_2	13.7	w_2	0.32	l_2	17.5	w_2	0.36
l_3	1.0	w_3	3.6	l_3	1.0	w_3	3.6
l_4	2.6	s	0.2	l_4	1.6	s	0.2

meet the criteria of the given in-band attenuation level and bandwidth by adjusting the three capacitances.

(vi) Finally, verify the performance, confirm the required range of values for C_1, C_2 and C_3 and optimise the design using a proper electromagnetic simulator. The optimised design is then fabricated using a suitable substrate and tested experimentally.

4 Results and discussions

To validate the proposed design procedure, two tunable filter prototypes are designed with centre frequency tunability from 0.5 to 1.5 GHz, and bandwidth from 50 to 150 MHz. Two prototypes are designed and built. Design #1 has the transmission zero f_{tz1} at upper side of the passband, whereas Design #2 has f_{tz1} at the lower side of the passband. The selected prototype filter for the design is second-order Chebyshev passband response that has a ripple of 0.1 dB and basic elements: $g_0 = 1$, $g_1 = 0.8431$, $g_2 = 0.622$, $g_3 = 1.3554$. The selected substrate for the designs is Rogers RO3003 with dielectric constant of 3 and thickness of 1.52 mm. The varactors used in the design are hyper abrupt junction tuning elements SMV1281 with tuning range from 0.6 to 14.2 pF and parasitic resistor R_s of 2.4 Ω. The simulation software advanced design system (ADS) is used in both schematic and layout design. After following the aforementioned design procedure, the optimised values of the design parameters are found to be: Design #1; $\theta_o = 24.6°$, $Z_{oe} = 166.8\ \Omega$, $Z_{oo} = 70.5\ \Omega$, $\theta_1 = 26.2°$, and $Z_1 = 100\ \Omega$; Design #2, $\theta_o = 28.7°$, $Z_{oe} = 172.4\ \Omega$, $Z_{oo} = 63.2\ \Omega$, $\theta_1 = 12.2°$, and $Z_1 = 100\ \Omega$. All the electrical lengths are calculated at the centre frequency of 1 GHz. The initial capacitance values in pF for C_1, C_2 and C_3 are: 1.3, 1.4, and 0.9, for Design #1; and 1.2, 3.0, and 4.2, for Design #2, respectively.

The configuration of the proposed tunable BPF is shown in Fig. 5*a*. Six varactors and three different voltage suppliers are required to control the performance of the filter. For easy design of the biasing circuit, two cascaded varactors C_{v3} with one common ground are used to represent C_3. Thus, the used value of C_{v3} is twice the calculated value of C_3. The biasing circuit is realised by DC biasing resistor R_{bias} with the value of 10 kΩ, and DC block capacitors C_{block} of 100 pF to block the DC signal. Once the initial dimensions are calculated assuming the use of a single-layer microstrip technique and using the well-known microstrip design equations [31], the simulation process is started with building the layout for the structure in ADS. To get accurate optimised results, SPICE models of the varactor diodes [32] are included using co-simulation method in both schematic and layout simulation in ADS. The final dimensions of two designs are listed in Table 1. Figs. 5*b* and *c* present photographs of the fabricated filters, which have overall sizes of 0.06 $\lambda_g \times 0.14\ \lambda_g$ and 0.06 $\lambda_g \times 0.16\ \lambda_g$ (λ_g is

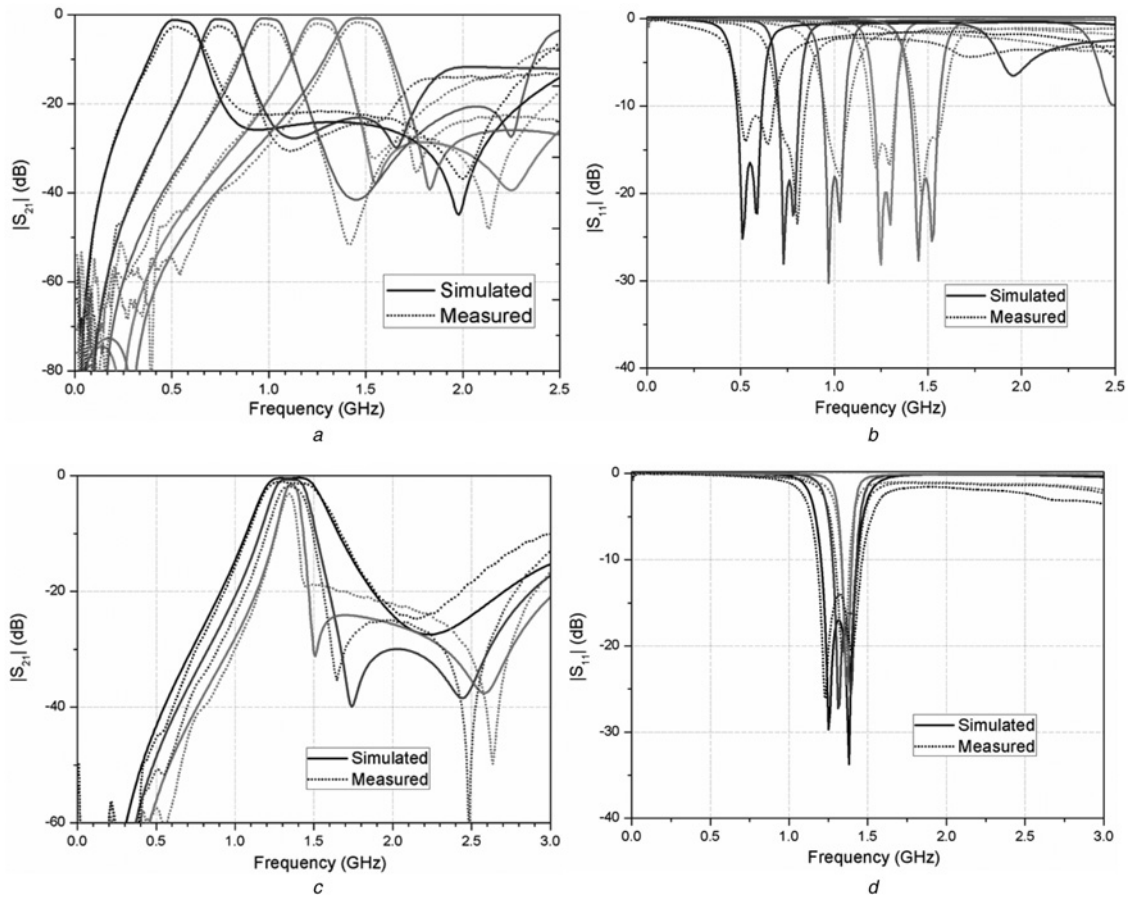

Fig. 6 *Measured and simulated results of centre frequency tunability of Design #1*

a $|S_{21}|$. (From low to high frequency, values of V_1, V_2 and V_3 are: 0.6, 1.4, 1.8; 3.8, 6.5, 3.2; 6.6, 12.6, 6.8; 10.2, 20.4, 10.2; 26, 26, 15.6, Unit: V.)
b $|S_{11}|$. (From low to high frequency, values of V_1, V_2 and V_3 are: 0.6, 1.4, 1.8; 3.8, 6.5, 3.2; 6.6, 12.6, 6.8; 10.2, 20.4, 10.2; 26, 26, 15.6, Unit: V.)
c $|S_{21}|$. (From narrow to wide band, values of V_1, V_2 and V_3 are: 26, 26, 10.2; 16.8, 24.5, 12.8; 9.6, 20.4, 26, Unit: V.)
d $|S_{11}|$. (From narrow to wide band, values of V_1, V_2 and V_3 are: 26, 26, 10.2; 16.8, 24.5, 12.8; 9.6, 20.4, 26, Unit: V.)

IET Microw. Antennas Propag., 2016, Vol. 10, Iss. 8, pp. 863–870

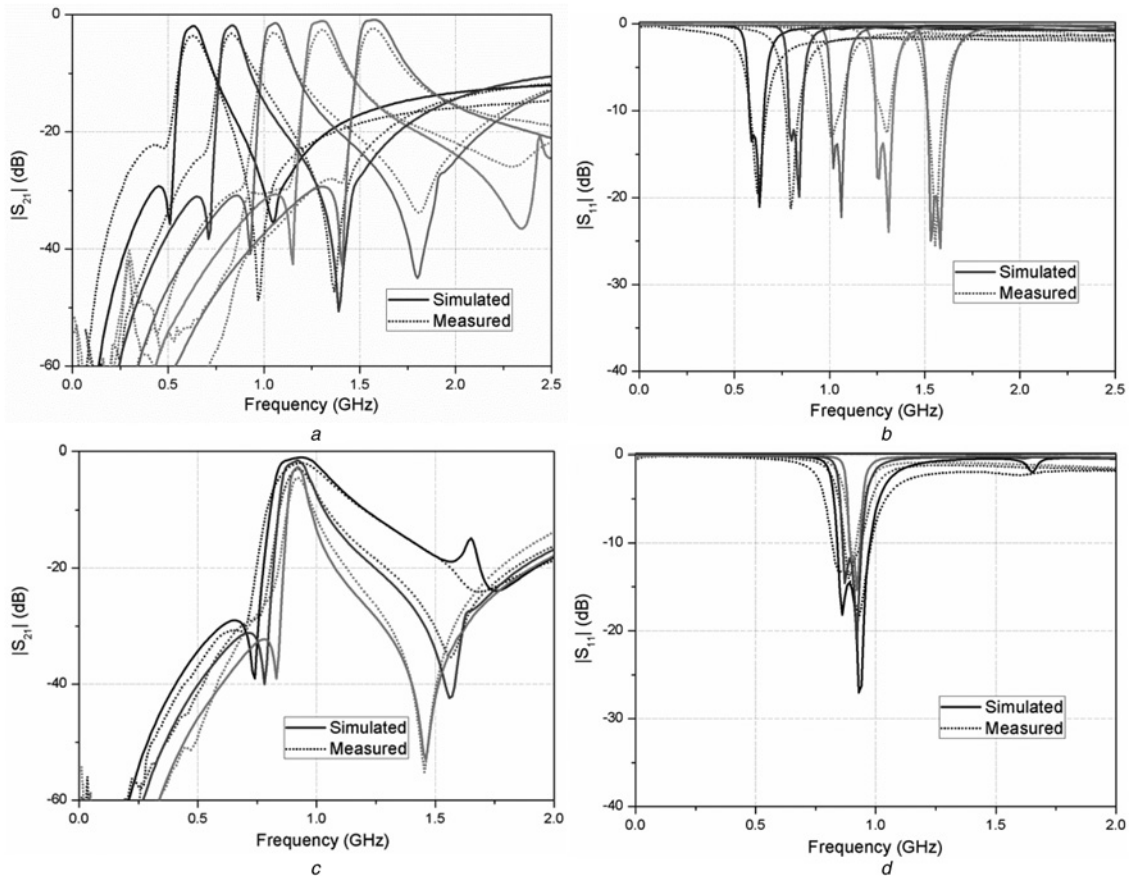

Fig. 7 *Measured and simulated results of centre frequency tunability of Design #2*

a $|S_{21}|$. (From low frequency to high frequency, values of V_1, V_2 and V_3 are: 4.6, 2.9, 1.1; 9.4, 5.7, 3.4; 15, 8.8, 5.6; 21.2, 14.6, 8.4; 26, 26, 12.4, Unit: V.)
b $|S_{11}|$. (From low frequency to high frequency, values of V_1, V_2 and V_3 are: 4.6, 2.9, 1.1; 9.4, 5.7, 3.4; 15, 8.8, 5.6; 21.2, 14.6, 8.4; 26, 26, 12.4, Unit: V.)
c $|S_{21}|$. (From narrow to wide band, values of V_1, V_2 and V_3 are: 14.8, 6.4, 4.5; 10.2, 6.9, 4.2; 7.8, 7.4, 3.6, Unit: V.)
d $|S_{11}|$. (From narrow to wide band, values of V_1, V_2 and V_3 are: 14.8, 6.4, 4.5; 10.2, 6.9, 4.2; 7.8, 7.4, 3.6, Unit: V.)

the guided-wavelength at the centre frequency 1 GHz), indicating that they are both compact designs. Besides, it is noted that in order to solder the tuning elements and biasing circuits properly, some extra microstrip patches that could work as transmission line with small electrical lengths are included in the layout, resulting in some effects on the performance of the filters.

The simulated and measured results of the filter are shown in Figs. 6 and 7, for Design #1 and Design #2, respectively. A comparison between the results of Design #1 with those for Design #2 clearly indicates the relocation of the transmission zero from the upper to the lower side of the passband. The measured results, which are in well agreement with the simulated, indicate that Design #1 and #2 have a wide tuning range for the centre frequency of 0.52–1.48 GHz (tuning ratio = 2.85) and 0.6–1.58 GHz (tuning ratio = 2.63), respectively. The results also show that Design #1 and #2 have a wide 3 dB bandwidth tunability of 55–285 MHz (tuning ratio = 5.2), and 45–190 MHz (tuning ratio = 4.2), respectively. These results meet the design objectives of the filter. The insertion loss for the two designs is between 1.2 and 3.5 dB for Design #1 and 1.8 to 4.3 dB for Design #2. Those results indicate that similar centre frequency tunability is achieved in the two designs. To verify the non-linear performance of the filters, the third-order intercept points (IIP_3) are calculated by using two input signals with 1 MHz separation. The IIP_3 points for Design # 1 and #2 are 6.8 and 8.4 dBm at 0.6 GHz, and 17.8 and 19.6 dBm at 1.4 GHz, respectively, when the bandwidth is fixed at 100 MHz for all the investigated cases. It is found that the IIP_3 increases when the operating centre frequency or bandwidth is increased due to the limited linearity of the diodes.

Table 2 Comparison between performance of the proposed tunable BPF and recently reported works

Ref.	Frequency tuning range, GHz	Frequency tuning range, %	3 dB bandwidth tuning range, MHz	3 dB bandwidth tuning range ratio	Insertion loss, dB	Size (guided wavelength)
[17]	1.5–2.2	37.8	50–170	3.4	3–6.5	0.25 × 0.18
[18]	1.55–2.1	30	40–120	3	4.5–6	0.28 × 0.19
[19]	2.9–3.5	18.8	134–402	3	1–3	0.38 × 0.35
[20]	0.43–0.6	33	0–52	–	1.4–4.4	0.14 × 0.1
[21]	0.6–1.45	83	120–950	7.9	1–3.5	0.23 × 0.16
[22]	1.16–1.4	18.8	120–210	1.8	3–5	0.19 × 0.19
[23]	0.59–0.91	42.6	115–315	2.7	1.2–1.6	0.42 × 0.14
[24]	0.52–1.42	93	90–320	3.6	1.6–3.9	0.08 × 0.07
[27]	1.16–1.4	18.8	120–210	1.8	3–5	0.25 × 0.25
this work #1	0.52–1.48	96	55–285	5.2	1.2–3.5	0.14 × 0.06
this work #2	0.6–1.58	90	45–190	4.2	1.8–4.3	0.16 × 0.06

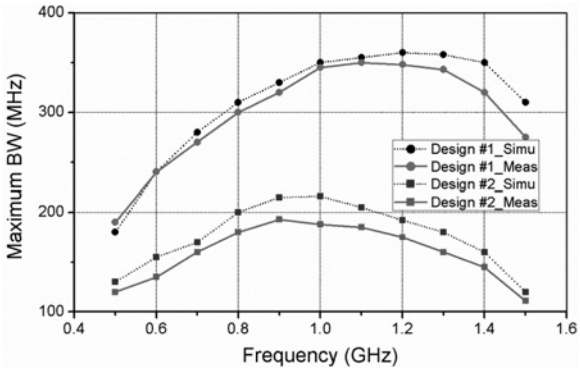

Fig. 8 *Variation of maximum achievable 3-dB bandwidth of two designs*

In general, good agreement between the measured and simulated results in the passband, cut-off band and locations of the transmission zeros can be observed. The slight differences, especially in the insertion losses where the measured are generally more than the simulated values, are thought to be due to the difference between the used SPICE models and realistic performance of the varactors, as well as the manufacturing tolerances. Some parasitic harmonics in the performance are caused by the added small patches for biasing circuit, the soldering process of the fabricated circuits and other manufacturing errors. Table 2 shows a comparison between the proposed tunable BPF and some other recently reported works. It is observed that the proposed structure has the widest centre frequency tuning range with a very decent bandwidth tuning range. Besides, the proposed design is more compact in size (only about $0.01\lambda_g^2$) compared with the previous works.

It is noted that the bandwidth tunability is not stable across the whole band range. This phenomenon is common in all of the band-tuned structures. As depicted in Fig. 8, the achievable bandwidth decreases when the centre frequency is too high or too low. This issue is caused by the fact that the coupling factor of the utilised coupled structure decreases at the lower and upper edges of the frequency band, which is the normal behaviour of traditional coupled structures. One possible solution to this issue is to use a broadside-coupled structure, which has almost constant coupling across an ultra-wide band [33].

5 Conclusion

A tunable BPF using a pair of short-ended stub-loaded resonators and short-ended coupled-line resonators has been presented. Using a varactor-loaded compact structure, the filter has been designed to realise a wide tuning range for the bandwidth and centre frequency. Moreover, the design enables a reconfigurable one-side passband edge transmission zero that can be relocated for sharp selectivity of the passband. Based on the even-odd mode analysis and a two-mode model circuit, a thorough design procedure has been presented and used to design two prototypes with different transmission zero location. The measured results indicate tuning range ratios for the centre frequency and bandwidth of up to 2.85 (0.52 to 1.48 GHz) and up to 5.2 (55 to 285 MHz), respectively. The proposed tunable BPF has great potential in modern multi-band and wireless telecommunication systems.

6 References

1 Hunter, I., Rhodes, J.: 'Electronically tunable microwave bandpass filters', *IEEE Trans. Microw. Theory Tech.*, 1982, **30**, (9), pp. 1354–1360

2 Brown, A., Rebeiz, G.: 'A varactor-tuned RF filter', *IEEE Trans. Microw. Theory Tech.*, 2000, **48**, (7), pp. 1157–1160

3 Haridasan, V., Lam, P., Feng, Z., *et al.*: 'Tunable ferroelectric microwave bandpass filters optimized for system-level integration', *IET Microw. Antennas Propag.*, 2011, **5**, (10), pp. 1234–1241

4 Zhu, H., Abbosh, A.: 'Tunable band-pass filter with wide stopband and high selectivity using centre-loaded coupled structure', *IET Microw. Antennas Propag.*, 2015, **9**, (13), pp. 1371–1375

5 Zhu, H., Abbosh, A.: 'Tunable balanced bandpass filter with wide tuning range of centre frequency and bandwidth using compact coupled-line resonator', *IEEE Microw. Wirel. Compon. Lett.*, 2016, **26**, (1), pp. 7–9

6 Tu, W.: 'Compact low-loss reconfigurable bandpass filter with switchable bandwidth', *IEEE Microw. Wirel. Compon. Lett.*, 2010, **20**, (4), pp. 208–210

7 Miller, A., Hong, J.: 'Wideband bandpass filter with reconfigurable bandwidth', *IEEE Microw. Wirel. Compon. Lett.*, 2010, **20**, (12), pp. 28–30

8 Chandler, S., Hunter, I., Gardiner, J.: 'Active varactor tunable bandpass filter', *IEEE Microw. Guided Wave Lett.*, 1993, **3**, (3), pp. 70–71

9 Rebeiz, G.: 'Low-loss 5.15–5.70 GHz RF MEMS switchable filter for wireless LAN applications', *IEEE Trans. Microw. Theory Tech.*, 2006, **54**, (11), pp. 3931–3939

10 Yan, W., Mansour, R.: 'Tunable dielectric resonator bandpass filter with embedded MEMS tuning elements', *IEEE Trans. Microw. Theory Tech.*, 2007, **55**, (1), pp. 154–160

11 Park, S., Rebeiz, G.: 'Low-loss two-pole tunable filters with three different predefined bandwidth characteristics', *IEEE Trans. Microw. Theory Tech.*, 2008, **56**, (5), pp. 1137–1148

12 Wang, X., Cho, Y., Yun, S.: 'A tunable combline bandpass filter loaded with series resonator', *IEEE Trans. Microw. Theory Tech.*, 2012, **60**, (6), pp. 1569–1576

13 Tang, C., Tseng, C., Chang, S.: 'A tunable bandpass filter with modified parallel-coupled line', *IEEE Microw. Wirel. Compon. Lett.*, 2013, **23**, (4), pp. 190–192

14 Athukorala, L., Budimir, D.: 'Open-loop tunable resonators and filters with constant bandwidth', *IET Microw. Antennas Propag.*, 2013, **7**, (6), pp. 800–806

15 Ni, J., Hong, J.: 'Varactor-tuned microstrip bandpass filters with different passband characteristics', *IET Microw. Antennas Propag.*, 2014, **8**, (6), pp. 415–422

16 Wong, P., Hunter, I.: 'Electronically reconfigurable microwave bandpass filter', *IEEE Trans. Microw. Theory Tech.*, 2009, **57**, (12), pp. 3070–3079

17 Chiou, Y., Rebeiz, G.: 'A tunable three-pole 1.5–2.2 GHz bandpass filter with bandwidth and transmission zero control', *IEEE Trans. Microw. Theory Tech.*, 2011, **59**, (11), pp. 2872–2878

18 Chiou, Y., Rebeiz, G.: 'Tunable 1.55–2.1 GHz 4-pole elliptic bandpass filter with bandwidth control and rejection for wireless systems', *IEEE Trans. Microw. Theory Tech.*, 2013, **61**, (1), pp. 117–124

19 LacorteCaniato Serrano, A., SaleteCorrera, F., Vuong, T., *et al.*: 'Synthesis methodology applied to a tunable patch filter with independent frequency and bandwidth Control', *IEEE Trans. Microw. Theory Tech.*, 2012, **60**, (3), pp. 484–493

20 Tsai, H., Chen, N., Jeng, S.: 'Center frequency and bandwidth controllable microstrip bandpass filter design using loop-shaped dual-mode resonator', *IEEE Trans. Microw. Theory Tech.*, 2013, **61**, (10), pp. 3590–3600

21 Mao, J., Choi, W., Tam, K., *et al.*: 'Tunable bandpass filter design based on external quality factor tuning and multiple mode resonators for wideband applications', *IEEE Trans. Microw. Theory Tech.*, 2013, **61**, (7), pp. 2574–2584

22 Tang, H., Chen, J., Zhou, L., *et al.*: 'Tunable dual-mode microstrip patch resonators and filters', *IET Microw. Antennas Propag.*, 2013, **7**, (6), pp. 408–414

23 Luo, X., Sun, S., Staszewski, R.: 'Tunable bandpass filter with two adjustable transmission poles and compensable coupling', *IEEE Trans. Microw. Theory Tech.*, 2014, **62**, (9), pp. 2003–2013

24 Zhu, H., Abbosh, A.: 'Compact tunable bandpass filter with widetuning range using ring resonator and short-ended coupled lines', *Electron. Lett.*, 2015, **51**, (7), pp. 568–570

25 Peng, H., Wu, L., Yin, W., *et al.*: 'Compact tunable bandpass filter with a fixed out-of-band rejection based on Hilbert fractals', *IEEE Trans. Compon. Packag. Manuf. Technol.*, 2013, **3**, (3), pp. 391–400

26 Long, J., Li, C., Cui, W., *et al.*: 'A tunable microstrip bandpass filter with two independently adjustable transmission zeros', *IEEE Microw. Wirel. Compon. Lett.*, 2011, **21**, (2), pp. 74–76

27 Tsai, H., Huang, B., Jeng, S.: 'A reconfigurable bandpass filter based on a varactor-perturbed, T-shaped dual-mode resonator', *IEEE Microw. Wirel. Compon. Lett.*, 2014, **24**, (5), pp. 297–299

28 Guyette, A.: 'Intrinsically switched varactor-tuned filters and filter banks', *IEEE Trans. Microw. Theory Tech.*, 2012, **60**, (4), pp. 1044–1056

29 Gómez-García, R., Guyette, A.: 'Reconfigurable multi-band microwave filters', *IEEE Trans. Microw. Theory Tech.*, 2015, **63**, (4), pp. 1294–1307

30 Hong, J., Lancaster, M.: 'Microstrip filters for RF/microwave applications' (Wiley, New York, 2001)

31 Abbosh, A.: 'Analytical closed-form solution for different configurations of parallel-coupled micro strip lines', *IET Microw. Antennas Propag.*, 2009, **3**, (1), pp. 137–147

32 'Skyworks SMV datasheets' (Skyworks solutions, Sunnyvale, CA, 2011)

33 Abbosh, A., Bialkowski, M.: 'Design of compact directional couplers for UWB applications', *IEEE Trans. Microw. Theory Tech.*, 2007, **55**, (2), pp. 189–194